Shimada, Tomonori; Watanabe, Yasuharu; Yokoyama, Hiroshi

Basic Study on Sediment Behavior in the Chiyoda Experimental Channel

BASIC STUDY ON SEDIMENT BEHAVIOR IN THE CHIYODA EXPERIMENTAL CHANNEL

Tomonori Shimada[1] Yasuharu Watanabe[2] and Hiroshi Yokoyama[3]

[1]Researcher, Civil Engineering Research Institute for Cold Region, PWRI
Hiragishi 1-3-1-34, Toyohira-ku, Sapporo, 062-8602, Japan, e-mail:t-shimada@ceri.go.jp
[2]Professor, Laboratory of River Disaster Prevention System, Kitami Institute of Technology
Koen-cho 165, Kitami, 090-8507, Japan, e-mail:y-watanb@mail.kitami-it.ac.jp
[3]Senior Researcher, Civil Engineering Research Institute for Cold Region, PWRI
Hiragishi 1-3-1-34, Toyohira-ku, Sapporo, 062-8602, Japan, e-mail:yokoyam@ceri.go.jp

ABSTRACT

The Chiyoda Experimental Channel of the Tokachi River is Japan's first full-scale experimental river channel in which experiments using artificial floods can be conducted in running water with a flow rate of up to 170m^3/s. The channel enables confirmation and clarification of phenomena that previously required consideration to the time, particle size and other scale effects in laboratory tests or were impossible or very difficult to observe in actual rivers. While full-scale experiments are scheduled to start in 2009, preliminary tests to ascertain the channel's properties were carried out in 2007 when it was put into service. This paper uses the results of these experiments to verify matters that could not be fully observed or understood on site as well as existing theories (sand waves, bedload) obtained in laboratory tests and by other means.

Key Words : *Chiyoda Experimental Channel, Dune, Bedload*

1. INTRODUCTION

The Ministry of Land, Infrastructure, Transport and Tourism's Hokkaido Regional Development Bureau planned the establishment of the Chiyoda New Channel in the Tokachi River (a Class A Hokkaido river) with the aim of improving the safety level of flood control. The channel, which has four tilting gates, is the largest of its kind in Japan, and has been in operation since April 2007(**Fig-1**). The Chiyoda Experimental Channel of the Tokachi River shown in **Fig-2** is a part of the Chiyoda New Channel, and is Japan's first full-scale experimental river channel in which experiments using artificial floods can be conducted in running water with a flow rate of up to 170 m^3/s.

Since the hydraulic conditions, data and time of running water and other conditions for experiments can be set to a certain extent, observation methods can be considered and prepared sufficiently in advance. The channel thus enables confirmation and clarification of phenomena that previously required consideration to the time, particle size and other scale effects in laboratory tests or were impossible or very difficult to observe in actual rivers. Full-scale experiments are scheduled to start in 20009. Preliminary tests are being carried out in 2007 and 2008 to clarify the channel's main properties and provide basic data for future experiments.

This paper first presents the main observation results obtained from the preliminary tests in 2007. It then uses these results to verify matters that could not be fully observed or understood on site, as well as existing theories (sand waves, bedload) obtained in laboratory tests and by other means, through optimum use of the full-scale experimental channel's merits.

2. Experimental overview

Table-1 lists the experimental specifications. It shows a summary of the observation results obtained in the upstream section of the Chiyoda Experimental Channel, which will be described in later sections of this paper. The water running time for each case was approximately seven hours.

Fig-3 displays the observation site where the different devices were used. A summary of each observation method is given below.

Table 1 Hydraulic quantities in each experimental case

	$Q[m^3/s]$	$h[m]$	$u[m/s]$	Fr	I_b	I_w	n	$u_*[m/s]$	Re_*	τ_*	τ_{*c}
Case1(first half)	33.87	0.67	1.61	0.63	1/518	1/514	0.021	0.11	*	*	*
Case1(second half)	109.74	1.47	2.26	0.59	1/518	1/515	0.024	0.16	*	*	*
Case2	54.53	0.94	1.82	0.60	1/512	1/503	0.023	0.13	1,775	0.059	0.050
Case3	21.19	0.53	1.29	0.57	1/505	1/493	0.022	0.10	1,337	0.032	0.050
Case4	16.04	0.44	1.18	0.57	1/513	1/491	0.020	0.09	1,453	0.026	0.050
Case5(first half)	15.83	1.27	0.64	0.69	1/518	1/488	0.018	0.09	1,163	0.024	0.050
Case5(second half)	6.15	0.25	0.82	0.53	1/518	1/493	0.021	0.07	903	0.015	0.050

Q: flow rate (result of high-water discharge observation using a float), h: mean water depth, u: mean flow velocity calculated from the flow rate and cross-sectional area of flow, Fr: Froude number, I_b: slope of the riverbed, I_w: slope of the water surface, n: coefficient of roughness calculated using Manning's mean velocity formula, u_*: friction velocity, Re_*: particle Reynolds number for the mean particle size of the riverbed, τ_*: dimensionless tractive force, τ_{*c}: dimensionless critical tractive force for the mean particle size of the riverbed * Data of Re_* and subsequent items are missing for Case 1 since no bed material survey was conducted.

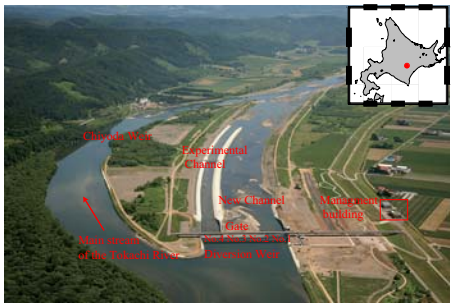

Figure 1 Chiyoda New Channel and Experimental Channel

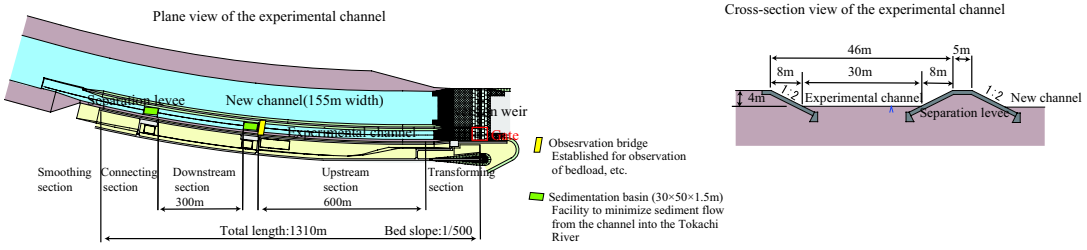

Figure 2 Overview of the Chiyoda Experimenatl Channel

2.1 Water level observation

The fixed-point water gauge collected data every 5 seconds, and processed the average for each 60-second period as one unit of data. The diver-type gauge also collected data every 5 seconds and used 60-second averages except for Case 1, where the momentary value measured at one-minute intervals was handled as one unit of data.

2.2 Flow rate observation

(1) High- and low- water discharge observation

High-water discharge observation using a float was conducted for six sections in the transverse direction, and low-water discharge observation using a roating-type current meter was conducted for ten sections in the transverse direction using the two-point method.

(2) ADCP observation

Two types of observation were conducted using ADCPs - one with a radio-controlled boat (referred to below as an RC boat) and another with a pole-type observation boat (pole wire-type) as shown in **Fig-4**. Both the RC boat and pole wire-type were equipped with echo-sounders, and performed

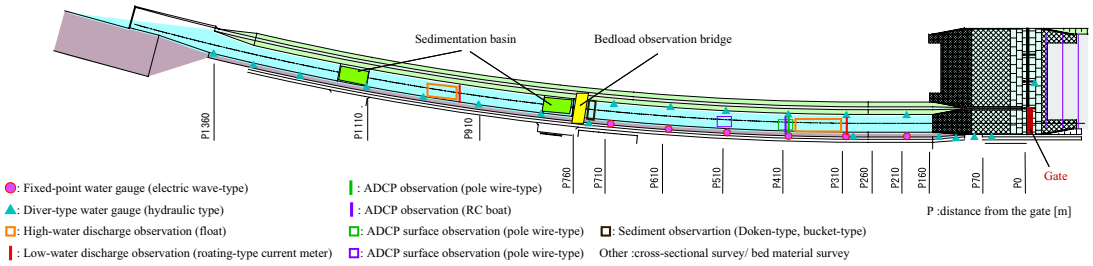

Figure 3 Observation site

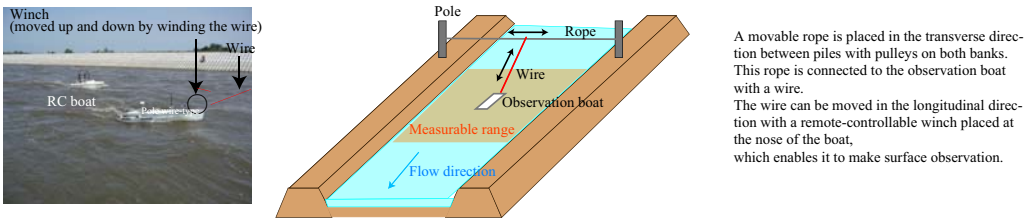

Figure 4 Pole wire-type ADCP observation

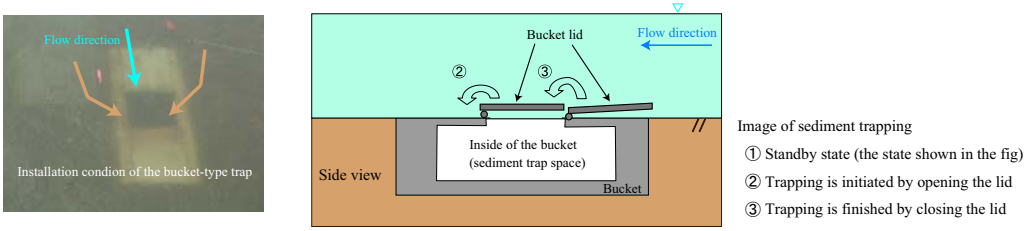

Figure 5 Bucket-type bedload trap

observation using the Real-time Kinematic Global Positioning System (RTK-GPS) to improve positional accuracy. For flow direction/velocity measurements, ADCPs (Workhorse Sentinel 1200 kHz, RE Instruments) were used (layer thickness: 0.1m, number of pings: 3, number of modes: 12[high-rate pinging mode]).

In Case 2, observation was conducted on three traverse lines in the vertical direction between the observation range of P450 and P430 for the pole wire-type and P500 and P525 for the RC boat to ascertain surface phenomena. The traversing positions were the center of the river channel and 10 m to the left and right of the center.

2.3 Riverbed height/ bed material

Cross-sectional and bed material surveys were conducted before and after running water. The cross-sectional survey was carried out at intervals of 50 m in the longitudinal direction, while the bed material survey was carried out at intervals of 50 m in the longitudinal direction, while the bed material survey was implemented at nine points in total -three points (left bank, center and right bank) on each of the three traverse lines (P260, P460 and P660).

2.4 Bedload

For bedload observation, Doken Type II (referred to below as Doken-type) and bucket-type bedload traps (bucket-type) were used. As shown in **Fig-5**, the bucket-type is a box-shaped bucket buried in the riverbed, and sediment is trapped by opening and closing the lid using a rope connected to it. Soil analysis was conducted for all the collected sediment.

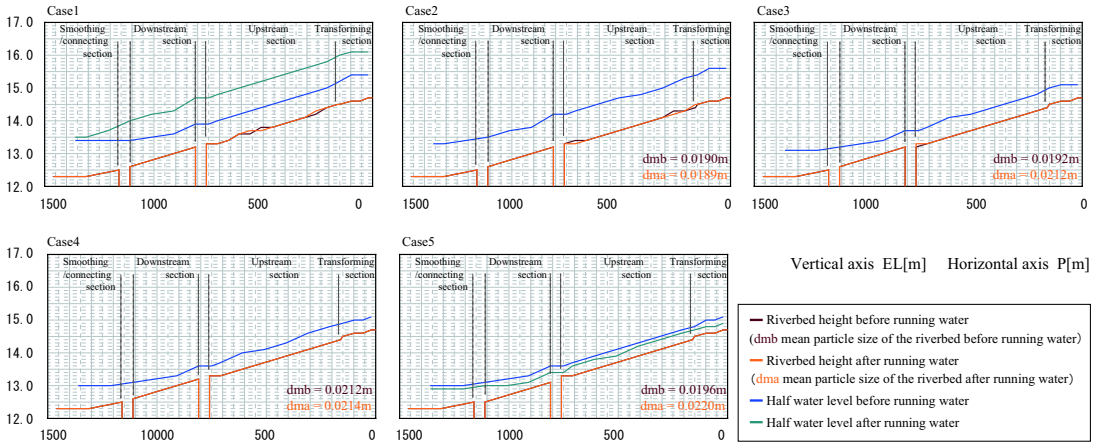

Figure 6 Water level observation results

3. Experimental results

3.1 Water level/surface shape

Fig-6 displays water surface shapes found by averaging the water levels of the hours when the flow conditions were stable. It can be seen that the water depth was almost uniform in the upstream section after passing through the transforming section. However, the backwater effect of the main stream was observed in the downstream was observed in the downstream was observed in the downstream section. The upstream section was therefore considered sufficiently functional as an experimental channel. It was also deemed possible to compare the results of flow rate observation using different observation methods (to be described below) on the assumption that the hydraulic conditions were uniform even though the observation points were different.

3.2 Flow rate

Because of its simplicity and certainty, high-water discharge observation using a float is the most common method under flooding and other harsh conditions. Methods using a roating-type current meter for low-water conditions and an RC boat equipped with an ADCP have also been presented in recent years. This section clarifies the differences in flow rate by observation method.

Fig-7 presents a comparison of flow rates by observation method, using high-water discharge observation as a benchmark. The flow rates shown here are mean values of the hours when the water level in each case was stable in the upstream section. In the entire range of observed flow rates, the results of low-water discharge observation corresponded mostly with the results of high-water discharge observation using a flow. While an ADCP was used for the observation, results were obtained only for the Point-Positioning Global Positioning System (PP-GPS) a single location in some hours since no RTK-GPS was obtained due to a GPS failure during observation. When the flow scale was small, most of the flow rates were calculated by interpolation (first-layer flow velocity value on the water surface: constant, theoretical formula on the riverbed: power curve fit) since the water was shallow and data were obtained only for one layer in the depth direction. In the case of a small flow rate of a PP-GPS, the difference from the high-water discharge observation was greater. In other cases, the difference was around -15%.

Kinoshita also summarized observation data of approximately 120 cases, and reported that the flow rates observed using an RC boat were -15 to -5 % of those in cases using a float.

In flow rate observation using a float, the value found by multiplying the obtained flow velocity by the coefficient of float is used as the mean flow velocity to find the flow rate. As the law of logarithmic flow velocity distribution is assumed here, the observation results obtained using a float may include errors if the flow velocity distribution deviates considerably from this law. This will be discussed in the section on sand waves below.

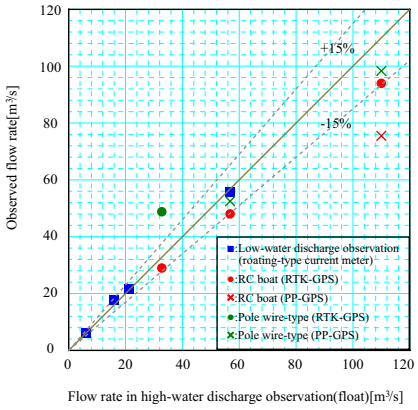

Figure 7 Comparison of flow rates by observation method

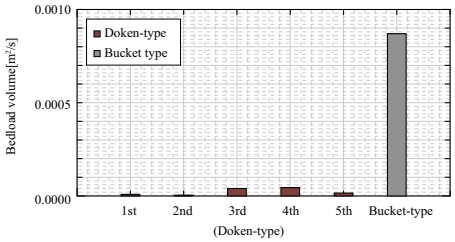

Figure 8 Bedload volume observation results

3.3 Bedload volume

Doken-type and bucket-type bedload observation was conducted for Case 2 and subsequent cases. It can be seen from **Table-1** that theoretical changes in the mean particle size occurred only in Case 2.

Here, the values found using the bucket-type are much larger than those of the Doken-type. The bedload volume is the sediment throughput per unit width. As indicated by the arrows in the photo shown in **Fig-5**, sediment also fell in from the sides of the bucket when the water was running. This is thought to be one of the reasons for the trapping of an excessive amount of sediment. The results of the Doken-type were therefore used as the true values in this study.

4. Examination of sand waves

4.1 Riverbed form

Fig-9(Left) is a classification map of small-scale riverbed forms by Ashida and Michiue. It can be seen from the figure that Case 3 and later were no-motion ranges, and that Case 2 was a lower-regime range (ripple, dune). The wavelength and wave height of ripples depend mainly on soil particle size, and were not observed under conditions when the particle Reynolds number was 20 or larger and the soil particle size was over 0.6 mm. It was therefore presumed that dune were created in this experiment.

Next, it was determined whether medium-scale sand waves were generated in Case 2. To ascertain this, the classification map of medium-scale riverbed forms by Kuroki and Kishi (**Fig-9(Right)**) was used. It can be seen from this that Case 2 was in a single-row sandbar range. It was then confirmed whether a sandbar was formed while water was running in the experiment. Fujita et al. expressed the sandbar development time T_e in a steady flow field by Eq.(1).

$$T_e = \frac{6\frac{B}{2}Z_{be}}{q_b} \tag{1}$$

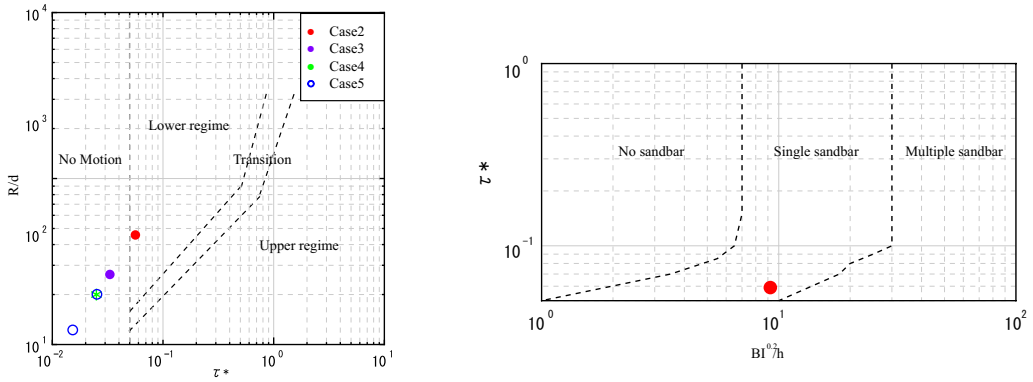

Figure 9 Left;Classification of a small-scale riverbed form, Right;Classification of medium-scale riverbed form

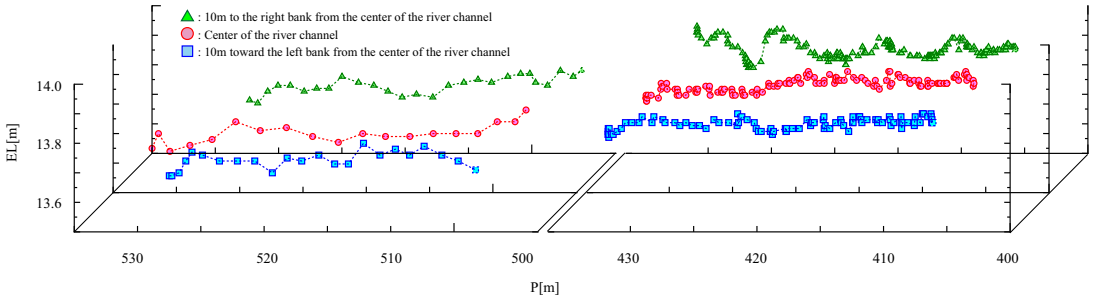

Figure 10 Riverbed height measurement using an ADCP

Where B is the river width, Z_{be} is the equilibrium sandbar height and q_b is the bedload volume per unit width. Calculating Z_{be} and q_b enables calculation of the sandbar development time.

Ikeda et al. expressed the equilibrium sandbar height Z_{be} by Eq.(2).

$$Z_{be} = 9.34h\left(\frac{2\frac{B}{2}}{d_m}\right)^{-0.45}\exp\left(2.53\mathrm{erf}\frac{\log_{10}2\frac{B}{2}/h - 1.22}{0.594}\right) \tag{2}$$

Where h is the water depth and d_m is the mean particle size of the riverbed.

Ashida and Michiue expressed the bedload volume per unit width q_b for the mean particle size by Eq.(3).

$$q_b = 17\tau_*^{3/2}\left(1-\frac{\tau_{*c}}{\tau_*}\right)\left(1-\frac{u_{*c}}{u_*}\right)\sqrt{sgd_m^3} \tag{3}$$

Where τ_*' is the non-dimensional effective tractive force, u_{*c} is the critical friction velocity, s is the specific gravity of sediment in the water and g is the acceleration of gravity.

The sandbar development time found using these equations was approximately 1,300 hours. This is much longer then the water running time of seven hours in Case 2. It can therefore be considered that no medium-scale sand waves were generated this time.

From the above results, it was presumed that a sand bank of small-scale sand waves existed in the riverbed form of Case 2 while water was running.

Surface observation using an RC boat and the pole wire-type was then conducted in Case 2. **Fig-10** displays the observation results, which are for a PP-GPS only due to a GPS failure. Generation of a dune can be observed as estimated from the above theory. Under the current hydraulic conditions, the theoretical wavelength was around 4.6 to 6.5 m, and the wave height was around 0.14 to 0.39 m. In the observation results, these values were around 7 m and 0.1 m, respectively.

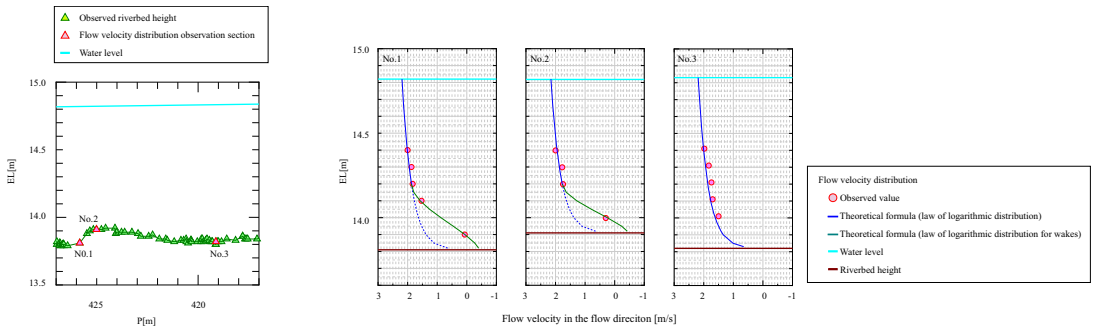

Figure 11 Flow velocity distribution in the vertical direciton on the dune (comparison between observed and theoretical values)

4.2 Flow velocity distribution above sand waves

This section examines the flow velocity distribution in the depth direction on the dune. Used as an example is the case of the right bank where pole wire observation (with which a dune can be confirmed more clearly) was carried out. As shown to the left of **Fig-11**, the three sections marked in red - No.1 (the flow directly under the dune crest), No.2 (the dune crest) and No.3 (the back of the dune) between P417 and P427 - were examined.

The law of logarithmic distribution for the general flow velocity in an open channel is expressed by Eq.(4).

$$\frac{u_{(z)}}{u_*} = Ar + \frac{1}{\kappa} ln \frac{z}{k_s} \tag{4}$$

Where z is the distance from the riverbed, u_z is the flow velocity at z, Ar is 8.5 (rough surface), κ is the Karuman constant (0.4), z is the water depth and k_s is the equivalent roughness (0.043 in this case, obtained by calculating backward using the hydraulic quantity and other conditions in **Table-1**).

Fig-11 presents the flow velocity distributions found from the observed values and the law of logarithmic distribution. While the distributions were almost identical in No.3, the observed values deviated greatly from the law of logarithmic distribution at deeper water levels in Nos. 1 and 2. This was thought to be caused by the creation of wakes by the dune. The lowest level in the range where the observed values corresponded mostly with the law of logarithmic distribution was assumed to be the midpoint. At levels lower than this midpoint, the bar-type roughness flow model (Eq.eq:山岡式)) of Yamaoka et al. was applied as the law of logarithmic distribution for wakes.

$$\frac{u_{(z)}}{U_1} = 1 - 0.313 C_x \left(\left(\frac{z}{b} \right)^{3/2} - 1 \right)^2 \tag{5}$$

Where U_1 is the flow velocity at the connecting point of the law of logarithmic distribution at the midpoint, C_x is the constant of flow velocity distribution (3.98 in this case, obtained by calculating backward using the observed flow velocity in layers lower than the midpoint), and b is the distance between the riverbed and midpoint.

As shown in **Fig-11**, close correspondence with the observed values was achieved by the application of Yamaoka's formula (i.e. the law of logarithmic distribution for wakes) to levels lower than the midpoint of the dune.

It is therefore assumed that the use of the law of logarithmic distribution is effective when a dune is generated and there is a midpoint in the flow velocity distribution.

4.3 Flow rate calculation taking wakes into account

When a dune was generated, the flow velocity distribution in the depth direction could not be described using only the law of logarithmic distribution. It was confirmed that the law of logarithmic

distribution for wakes must also be considered. The results of flow rate observation using the methods outlined above were therefore compared, and the differences between the results of high-water discharge observation and those of flow rate observation were found using an ADCP. These results were examined using the flow velocity distribution in the depth direction.

In high-water discharge observation, floats are selected depending on the water depth, and the flow rate is calculated by assuming that the law of logarithmic distribution is valid and finding the mean flow velocity using the coefficient of float. The flow rate calculated using a float may therefore include errors if the flow velocity distribution deviates considerably from the law of logarithmic distribution. This will be discussed in the section on dune below. This is partly because of the difficulty in assuming the vertical distribution curve of the flow velocity, as well as the problems inherent in comparing an indoor experimental channel and an actual river.

In the experiment in the Chiyoda Experimental Channel, flow rate was observed using a float and an ADCP, the dune form was observed using an ADCP, and the flow velocity distribution above the dune was obtained. Based on these results, the flow rate per unit width was calculated and compared for the case assuming the law of logarithmic distribution and the case deviating from the law and taking wakes and other conditions into account. The flow rate per unit width was found using Eq.(6).

$$q = \int_0^h u_{(z)} dz \tag{6}$$

Where q is the flow rate per unit width. As an example, this equation was used for No.1 in **Fig-11**, which was a wake section. The flow rate per unit width was 1.99 m^2/s when the value for the law of logarithmic distribution was used. When the influence of a dune was taken into account and the value for the law of logarithmic distribution for wakes was used, the rate was 1.72 m^2/s, which was approximately 86.6% that of the case where only the value for the law of logarithmic distribution was used. This corresponded closely with the results of flow rate observation in this study (the flow rate observed using an ADCP was -15 % of the value of high-water discharge observation). Although this involved comparison using partial results of one case of flow conditions, it can be said that it revealed one cause of the difference in results of high-water discharge observation and flow rate observation using an ADCP.

5. Examination of bedload volumes

This section presents a comparison between the observation results of bedload volumes outlined above and existing theoretical bedload formulas to find a formula applicable to the Chiyoda Experimental Channel.

5.1 Existing bedload volume formulas

Many formulas have been presented for bedload calculation. Bedload motion is a complex phenomenon that occurs in the very thin layer near the boundary between the flowing water and the riverbed. Bedload formulas are thus derived by modeling the motion mechanism of drifting sand or using a dimensional analysis method. In this study, the volume of bedload by particle size was calculated using the Meyer Peter-Müller formula as a dimensional analysis model, the Ashida-Michiue formula as a drag model and the Sato-Kikkawa-Ashida formula as a lift model. At this time, the effective tractive force was taken into account on the assumption that a dune was formed on the experimental channel as mentioned before. The bedload volume formula by particle size is as expressed below.

The Ashida-Michiue formula is expressed by Eq.(8).

$$q_{bi} = 17 p_i \tau_{*i}^{3/2} \left(1 - \frac{\tau_{*ci}}{\tau_{*i}}\right) \left(1 - \frac{u_{*ci}}{u_*}\right) \sqrt{sgd_i^3} \tag{7}$$

$$\tau'_{*i} = 0.21 \tau_{*i}^{1/2}$$

Where d_i is the soil particle size, and subscript i is the physical quantity for particle size d_i in mixed grain size (used commonly for all the symbols shown below). Also, q_{bi} is the bedload volume by

particle size, p_i is the rate of particles with a particle size of d_i on the riverbed, s is the specific gravity of sediment in the water, g is the acceleration of gravity, τ'_{*i} is the non-dimensional effective tractive force by particle size, τ_{*ci} is the non-dimensional critical tractive force ($= u_*^2/sgd_i$), u'_* is the effective friction velocity, u_* is the friction velocity and τ_{*i} is the non-dimensional tractive force by particle size ($= u_{*ci}^2/sgd_i$). In this case, u_{*ci} (the critical friction velocity by particle size) is found using the Egiazaroff-Asada formula(Eq.(8)).

$$\frac{u_{*ci}^2}{u_{*cm}^2} = \left(\frac{\log 23}{\log\left(21\frac{d_i}{d_m} + 2\right)} \right)^2 \frac{d_i}{d_m} \tag{8}$$

The Sato-Kikkawa-Ashida formula is expressed by Eq.(10).

$$q_{bi} = p_i \frac{u_*^3}{sg} F\left(\frac{u_*^2}{u_{*ci}^2}\right) f_{(n)} \tag{9}$$

$$F\left(\frac{u_*^2}{u_{*ci}^2}\right) = \frac{1}{1 + 8\left(\frac{u_{*ci}^2}{u_*^2}\right)^4}$$

$$n \geq 0.025 \quad f_{(n)} = 0.623$$

$$n \leq 0.025 \quad f_{(n)} = 0.623(40n)^{-3.5}$$

The Meyer Peter-Müller formula is expressed by Eq.(11).

$$q_{bi} = 8p_i \left(\tau'_{*i} - \tau_{*ci}\right)^{1.5} \sqrt{sgd_i^3} \tag{10}$$

$$\tau'_{*i} = \frac{u_*^2}{sgd_i}$$

$$u'_* = \left(\frac{n_b}{n}\right)^{3/4} u_*$$

$$n_b = 0.0192 d_{90}^{1/6}$$

Where n_b is Stlickler's coefficient of roughness, d_{90} is the 90 % particle size of the particle size distirbution (the unit here is [cm]) and n is Manning's coefficient of roughness.

This section gives a brief summary of the characteristics of each bedload volume formula. The Ashida-Michiue and Sato-Kikkawa-Ashida formulas are designed to calculate the bedload volume by particle size in the case of mixed particle sizes. However, the Meyer Peter-Müller formula is originally intended for calculation of the total sand volume, and particle size is not taken into account. It was therefore modified to enable calculation by particle size (by introducing d_i, p_i, τ_{*ci}), and has been used widely as Eq.(10).

When comparing with the observed values in Case 2, it is necessary to consider the flow resistance caused by dune and incorporate an effective tractive force because of the above-mentioned dune formation. However, the Sato-Kikkawa-Ashida formula does not have a term to express the effective friction velocity and effective tractive force. Since $f_{(n)}$ includes the coefficient of roughness n, resistance by dune and bed material can be taken into consideration by finding n from the observation results.

5.2 Comparison between the obsreved values and existing bedload volume formulas

Fig-12(Right) presents the results of non-dimensional tractive force. The results indicate that the values found using the Ashida-Michiue and Sato-Kikkawa-Ashida formulas correspond mostly with the observed values, although the values of the Meyer Peter-Müller formula were too large.

Fig-12(Right) presents the results of a comparison of bedload volumes by particle size. It can be seen that, under the current experimental conditions, the bedload volume was overestimated by the Sato-Kikkawa-Ashida formula when the particle size was smaller. However, a tendency similar to that of the observation results was obtained by the Ashida-Michiue formula for a wide range of particle sizes.

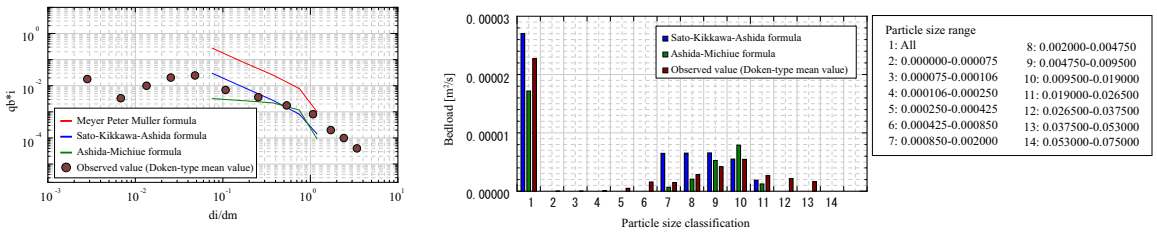

Figure 12 Left;Non-dimensional bedload volumes, Right;Sediment volume by particle size

From the above results, the Ashida-Michiue formula is considered the most appropriate for the hydraulic, bed material and other conditions of the Chiyoda Experimental Channel. However, this is a comparison of observation results in only one case. It will be necessary in the future to conduct observation and examination under various flow conditions. The variation in result found by different bedload volume formulas will also be studied in the future.

6. Conclusion

Although this year's experiments were conducted under low flow rate conditions due to low rainfall, the following findings were obtained from the observation results: 1) Area classification of sand waves can be applied on a full-scale basis. 2) There is a midpoint in the flow velocity distribution on the dune, and the distribution can be explained using the law of logarithmic distribution for wakes in sections deeper than this point. 3) Wakes created by the dune may affect flow rates observed using a float or an ADCP. 4) Since the Chiyoda Experimental Channel is a full-scale facility, the Ashida-Michiue formula can be applied as a bedload formula. In the future, it will be necessary to clarify phenomena for a wider range of flow rates by conducting experiments under high flow conditions.

REFERENCES

1) Tokachi River Chiyoda Experimental Channel, Obihiro Development and Construction Department, Hokkaido Regional Development Bureau, Ministry of Land, Infrastructure, Transport and Tourism, http://www.ob.hkd.mlit.go.jp/hp/kakusyu/chiyoda/zi/zi0.htm
2) Win River Operation Manual, SEA Corporation, pp.31, 2005.
3) E.g., Ryossaku KINOSHITA: A Flow Structure during Flooding Observed by an ADCP (acoustic Doppler current profiler), 51st Hydraulic Engineering Conference of the Japan Society of Civil Engineers, pp.12, 2007.
4) Kazuo ASHIDA and Masanori MICHIUE: A Basic Study of the Resistance of Moving Bed Flows and Bedloads, Journal of the Japan Society of Civil Engineers, No.206, pp.56-69, 1972.
5) Mikio KUROKI and Tsutomu KISHI: A Theoretical Study on the Classification of Medium-Scale Riverbed Forms, Journal of the Japan Society of Civil Engineers, No.342, 1984.
6) Yuichiro FUJITA et al.: Formation Process of a Braided Stream, 31st Hydrology Conference of the Japan Society of Civil Engineers, pp.695-700, 1987.
7) Shunsuke IKEDA et al.: The Dimensional Flow and Bed Topography in Sand Silt Meandering Rivers, Journal of the Japan Society of Civil Engineers, No.369, pp.99-108, 1986.
8) Hydraulic Formulas, Japan Society of Civil Engineers, p.183, 1999.
9) Hiroshi YOKOYAMA, Kazufumi KIZAWA and Kazuyoshi HASEGAWA: Relationship between Water Level Changes and Hydraulic Quantity during Flooding in the Mukawa RIver, Part 2, 55th Annula Conference of the Japan Society of Civil Engineers, pp.204-205, 2000.
10) Isao YAMAOKA: Effects of the Rectangular Roughness Elements of the River Bed upon the Resistance of the Channel, Civil Engineering Laboratory Report, No.27, 1962.
11) Hydrological Observation, Japan Construction Engineers' Association, p.165, 1996.
12) Meyer-Peter,E,and Müller,R.: Formulas for bed-load transport, Proc.2nd Cong. ITAH, Stockholm, Sweden, pp.39-64, 1948.
13) Seiichi SATO, Hideo YOSHIKAWA and Kazuo ASHIDA: A Study on Bedload Transport of Riverbed Gravel, Ministry of Construction Civil Engineering Laboratory Report, No.98, pp.13-31, 1958.
14) Egiazaroff,I.V. : Calculation of Nonuniform Sediment Concentrations, Proc.ASCE, vol.91,No.HY4, pp.225-247, 1965.
15) Tadashi SUETSUGU, Takaaki KUSAKABE and Susumu TANIGUCHI: Improvement of a Riverbed Fluctuation Model for Dynamic State Prediction of Sediment, material of the National Institute for Land and Infrastructure Management, No.69, pp.58-60, 2003.